 Open access • Journal Article • DOI:10.1061/(ASCE)0733-9429(1995)121:2(129)

Characteristics of undular hydraulic jumps. experimental apparatus and flow patterns — [Source link](#)

Hubert Chanson, J. S. Montes

Published on: 01 Feb 1995 - Journal of Hydraulic Engineering (American Society of Civil Engineers)

Topics: Hydraulic jumps in rectangular channels, Froude number, Momentum-depth relationship in a rectangular channel, Hydraulic jump and Jump

Related papers:

- [Characteristics of Undular Hydraulic Jumps: Experiments and Analysis](#)
- [Hydraulic condition for undular-jump formations](#)
- [Open channel flow](#)
- [Undular Hydraulic Jump](#)
- [Non-breaking undular hydraulic jump](#)

Share this paper:    

View more about this paper here: <https://typeset.io/papers/characteristics-of-undular-hydraulic-jumps-experimental-49nes4kko3>

CHANSON, H., and MONTES, J.S. (1995). "Characteristics of Undular Hydraulic Jumps. Experimental Apparatus and Flow Patterns." *Journal of Hydraulic Engineering*, ASCE, Vol. 121, No. 2, pp. 129-144. Discussion : Vol. 123, No. 2, pp. 161-164 (ISSN 0733-9429).

CHARACTERISTICS OF UNDULAR HYDRAULIC JUMPS. EXPERIMENTAL APPARATUS AND FLOW PATTERNS

by H. CHANSON¹ and J.S. MONTES²

Abstract : In open channels, the transition from supercritical to subcritical flows is called a hydraulic jump. For low upstream Froude numbers, free-surface undulations develop downstream of the jump and the hydraulic jump is called an undular jump. New experiments on undular hydraulic jumps were performed in a rectangular channel in which the upstream flows were fully developed turbulent shear flows. In this paper, the main flow patterns are described. Visual and photographic observations indicate five types of undular jumps. One of the main flow characteristics is the presence of lateral shock waves for Froude numbers larger than 1.2. The results show that the disappearance of undular jump occurs for Froude numbers ranging from 1.5 to 2.9 and that the wave length and amplitude of the free-surface undulations are functions of the upstream Froude number and the aspect ratio y_c/W .

INTRODUCTION

In open channel flow, the transition from a rapid to a tranquil flow is called a hydraulic jump. It is characterised by the development of large-scale turbulence, surface waves, energy dissipation and air entrainment. The flow conditions downstream of the jump are deduced from the momentum and continuity equations and the upstream flow conditions. For a horizontal rectangular channel of constant channel width, and neglecting the bed and wall friction, it can be shown that (STREETER and WYLIE 1981) :

$$\frac{h_2}{h_1} = \frac{1}{2} \left(\sqrt{1 + 8 Fr_1^2} - 1 \right) \quad (1)$$

$$\frac{Fr_2}{Fr_1} = \frac{2^{3/2}}{\left(\sqrt{1 + 8 Fr_1^2} - 1 \right)^{3/2}} \quad (2)$$

where the subscripts 1 and 2 refer respectively to the upstream and downstream flow conditions of the hydraulic jump (fig. 1) and Fr is the Froude number.

¹ Lecturer, Hydraulics and Fluid Mechanics, Department of Civil Engineering, The University of Queensland, Brisbane QLD 4072, Australia.

² Senior Lecturer, Department of Civil and Mechanical Engineering, The University of Tasmania, Hobart TAS 7000, Australia.

CHANSON, H., and MONTES, J.S. (1995). "Characteristics of Undular Hydraulic Jumps. Experimental Apparatus and Flow Patterns." *Journal of Hydraulic Engineering*, ASCE, Vol. 121, No. 2, pp. 129-144. Discussion : Vol. 123, No. 2, pp. 161-164 (ISSN 0733-9429).

The energy dissipation within a hydraulic jump can be derived from the energy equation using the above results (eq. (1) and (2)) :

$$\frac{\Delta H}{y_c} = \frac{(h_2 - h_1)^3}{4 h_1 h_2 y_c} \quad (3)$$

where ΔH is the head loss and y_c is the critical depth.

A hydraulic jump of low height is characterised by free surface undulations downstream of the jump (fig. 2) : it is called an undular jump. For an undular jump, the energy loss (eq. (3)) is very small but not zero. As the undular jump does not have a marked roller, the energy losses are radiated forward in a train of stationary waves (MONTES 1979, 1986). The undulations extend far downstream of the jump with decaying wave lengths, and can occupy a significant length of the channel.

Bibliographic review

Most hydraulic and fluid mechanics textbooks ignore the case of undular hydraulic jumps in their section on open channel flows. Some specialised textbooks (ROUSE 1938, CHOW 1959, HENDERSON 1966) indicate the occurrence of an undular jump for $Fr_1 < 1.7$ but do not detail its flow properties.

Some experimental studies of hydraulic jumps include some undular jump cases : e.g., BAKHMETEFF and MATZKE (1936), BINNIE and ORKNEY (1955), SANDOVER and HOLMES (1962). These researchers did not detail however the specific properties of undular jumps. Other researchers studied particularly undular jumps : LEMOINE (1948), SERRE (1953), IWASA (1955), JONES (1964), ANDERSEN (1978). But all of these analyses were based upon an analogy with an undular surge advancing in still water and the various results are sometimes conflicting.

MONTES (1979) showed that the analogy between undular jump and undular surge does not take into account the flow characteristics. In the case of undular jumps, turbulent boundary layers are partially or fully developed along both the channel bed and the sidewalls. Further as the jump extends over a great length, the assumption of negligible bottom and sidewall friction (used in undular surge calculations) is unrealistic.

FAWER (1937) performed an interesting study but his work was ignored by most researchers. This is despite FAWER detailing clearly the main features of undular hydraulic jumps.

Recently, MONTES (1986) and RYABENKO (1990) presented two pertinent and independent studies. Their results refuted the principle of an analogy between undular jump and undular surge. Further, they suggested that the transition between an undular jump and a weak jump may occur for upstream Froude numbers in the range 1.0 to 3.6, the transition being a function of the upstream flow conditions.

Undular jump flow situations

An undular hydraulic jump may occur in irrigation and water supply channels, in estuaries during some period of the tides, and in narrow or shallow straights subjected to strong currents.

CHANSON, H., and MONTES, J.S. (1995). "Characteristics of Undular Hydraulic Jumps. Experimental Apparatus and Flow Patterns." *Journal of Hydraulic Engineering*, ASCE, Vol. 121, No. 2, pp. 129-144. Discussion : Vol. 123, No. 2, pp. 161-164 (ISSN 0733-9429).

When an undular jump takes place in a channel, waves of large amplitudes develop and propagate downstream of the jump. These undulations may overtop and damage extensively the channel banks. The propagation of free-surface waves downstream of undular jumps must be taken into account for the design of canals and for the maintenance of natural channels. For natural channels and canals, the embankment height must be higher than the crest of the free-surface undulations to prevent the erosion and ultimately the destruction of the banks. Furthermore, the propagation of free-surface waves might impose additional impact loads, perturbations and vibrations on downstream structures (e.g. gates, locks or weirs). CHANDRAN and VENKATRAMAN (1985) described a case of an undular jump immediately upstream of pump intakes. The waves, induced by the jump, perturbed the pump operation with the result that the channel was modified to avoid the undular hydraulic jump. Also, the propagation of downstream waves over long distances might affect or prevent navigation in the channel.

Undular hydraulic jumps may occur also aft of ships travelling in canals and in shallow waters. HASLEWOOD (1985) presented a comprehensive study of the problem. The appearance of undular jumps coincides with a rapid increase in ship resistance in canals or shallow waters. The growth in ship resistance is attributed to the onset of critical conditions alongside the ship and the sudden apparition of undular jump waves aft of the ship.

New experimental data relating to free surface undulations downstream of an undular jump are presented herein (table 1). The experiments have been performed in a rectangular channel with fully developed upstream shear flow conditions. The results are compared with existing data, and the effects of channel width and bottom shear stress are discussed. Full details of the experimental data are given by CHANSON (1993).

EXPERIMENTAL APPARATUS

Experiments were performed in a 20-m long channel of uniform rectangular section made of glass (bottom and sidewalls), located in the Hydraulic Laboratory of the University of Queensland (fig. 2). The channel width is 0.25 m and the sidewall height is approximately 0.27 m. The channel is supported on an elevated steel truss which spans between main supports. The channel slope can be adjusted using a geared lifting mechanism.

Regulated flows are supplied from a constant head tank feeding an inlet transition to the channel via a butterfly valve mounted on the head tank discharge line. Tailwater levels are controlled by a radial gate fitted at the downstream channel end. The upstream face of the gate is covered by a dozen layers of 75%-shade cloth to prevent wave reflection from the gate. Further details on the channel were given by ISAACS and MACINTOSH (1988).

CHANSON, H., and MONTES, J.S. (1995). "Characteristics of Undular Hydraulic Jumps. Experimental Apparatus and Flow Patterns." *Journal of Hydraulic Engineering*, ASCE, Vol. 121, No. 2, pp. 129-144. Discussion : Vol. 123, No. 2, pp. 161-164 (ISSN 0733-9429).

In this study, the water discharge ranges from 2 to 30 L/s, the upstream Froude number is between 1.05 and 3.0, the aspect ratio y_c/W is in the range 0.075 to 0.455 and the channel slope ranges from 0.2 to 4.5 degrees.

Instrumentation

The water discharge is measured typically using a bend meter, installed in the discharge line from the constant head tank. For small discharges (i.e. $Q_w < 10$ L/s), the discharge can be measured also using a calibrated 300 L tank. The percentage error is expected to be less than 5%.

Longitudinal flow depths are measured using a rail mounted pointer gauge positioned over the centreline of the channel. The gauge is accurate within 0.5 mm. The flow depth measurements were the mean value over a period of one minute. The distance along the flume from the channel entrance is measured with a metre line; the error being less than 0.5 cm. The wave lengths and wave amplitudes were deduced from the free-surface profile measurements. Photographs were taken during the experiments and these were used to check the visual observations of the locations of the lateral shock waves, wave crests and wave bottoms.

The velocity, pressure and specific energy measurements were performed using a Pitot tube. The Pitot tube has an external diameter $\varnothing = 3.3$ mm and the pressure head at the tip is measured through a 1-mm diameter hole. The distance between the tip of the probe and the lateral pressure points ($\varnothing = 0.5$ mm) is 20 mm. During the experiments, the Pitot tube was connected to a 30-degree inclined manometer by two 2-m long hard nylon tubes (Nylex™ : outside $\varnothing = 6.35$ mm, inside $\varnothing = 4.32$ mm). The manometer consists of two identical glass tubes open to the atmosphere at the top end, and it was fixed at the same location for all measurements. The first pressure reading gives the total head while the second reading indicates the pressure head plus the elevation.

The translation of the Pitot tube in the direction perpendicular to the channel bottom is controlled by a fine adjustment travelling mechanism connected to a Mitutoyo™ digimatic scale unit. The error in the vertical position of the Pitot tube is less than 0.1 mm. The longitudinal translation of the Pitot tube is controlled manually : the Pitot tube and the digimatic scale unit are fixed to an L-shape aluminium beam clamped to the top of the channel. The error in the longitudinal location of the Pitot tube is less than 5 mm.

At a given cross-section and at a distance y from the channel bed, the local total head H , pressure P , velocity V and specific energy E can be deduced from the two manometer readings, the channel slope and the bed elevation.

Preparation of the experiments

During the experiments, the location of the hydraulic jump was controlled by the downstream gate, the channel slope and the discharge. The channel slope and the discharge control the quasi-uniform flow upstream of the jump while the downstream gate acts as a downstream control. Repetitions of the same

CHANSON, H., and MONTES, J.S. (1995). "Characteristics of Undular Hydraulic Jumps. Experimental Apparatus and Flow Patterns." *Journal of Hydraulic Engineering*, ASCE, Vol. 121, No. 2, pp. 129-144. Discussion : Vol. 123, No. 2, pp. 161-164 (ISSN 0733-9429).

experiments over several different days indicated that the location of the start of the undular jump could be controlled to within about ± 10 mm.

For all of the experiments, the start of the undular jump was located at a distance from the channel entrance of between 9.5 and 15 m. For the upstream flows, the boundary layer was fully-developed and the boundary layer thickness was equal to the flow depth.

Upstream flow conditions

The main upstream flow characteristics were investigated 10.9 m downstream of the channel entrance for discharges ranging from 2 to 30 L/s and Froude numbers between 1.1 and 2.4. During the experiments, the friction factor was deduced from uniform flow measurements performed in the channel before the establishment of the undular jump. For the present series of experiments, the friction factor f ranges from 0.015 up to 0.026. These values correspond to an equivalent surface roughness k_s between 0.01 to 0.15 mm. For the same channel, ISAACS and MACINTOSH (1988) deduced $k_s = 0.05$ mm for a water discharge $Q_w = 20$ L/s and a slope of 0.11 degrees.

For all of the experiments, the upstream centreline velocity distributions show that the bottom turbulent boundary layer reached the free-surface upstream of the measurement location. Typical examples are shown on figure 3. All the data show clearly that the boundary layer was fully-developed for all investigated flow conditions. At the measurement location (i.e. $x = 10.9$ m), the velocity distribution can be approximated by a power law :

$$\frac{V}{V_{\max}} = \left(\frac{y}{h}\right)^{1/N} \quad (4)$$

where V_{\max} is the maximum velocity at the free-surface (on the centreline), y is the distance measured perpendicular to the channel bottom and h is the flow depth. The results (CHANSON 1993) indicate that the exponent N ranges from 6.9 to 8.8. For uniform flows, CHEN (1990) derived a theoretical relation between the exponent N of the power law velocity distribution and the friction factor f as :

$$N = K \sqrt{\frac{8}{f}} \quad (5)$$

where K is the Von Karman constant ($K = 0.4$). A comparison shows a good agreement between the values of N deduced from the data and the predictions of equation (5).

A detailed analysis of the upstream flow conditions indicates that the ratio of the mean velocity on the centreline $(V_m)_{CL}$ to the mean flow velocity $Q_w/(W h)$ ranges from 1.05 to 1.35, where W is the channel width. These values suggest that the three-dimensional effects of the lateral boundary layers on the sidewalls are not negligible.

The analysis of the pressure distributions at $x = 10.9$ m shows clearly that the centreline pressure distribution upstream of an undular jump is perfectly hydrostatic.

CHANSON, H., and MONTES, J.S. (1995). "Characteristics of Undular Hydraulic Jumps. Experimental Apparatus and Flow Patterns." *Journal of Hydraulic Engineering*, ASCE, Vol. 121, No. 2, pp. 129-144. Discussion : Vol. 123, No. 2, pp. 161-164 (ISSN 0733-9429).

CHARACTERISTIC FLOW PATTERNS

Classification of undular jumps

Visual and photographic observations indicate five types of undular jumps (fig. 4) :

- *Type A* : $1 \leq Fr_1 \leq Fr^A$

For Froude numbers slightly above unity, free surface undulations of small amplitude and relatively long wave length develop. The flow is two-dimensional. No roller or shock waves are visible.

- *Type B* : $Fr^A \leq Fr_1 \leq Fr^B$

With an increase of the upstream Froude number, lateral shock waves start to develop upstream of the first wave crest. The shock waves intersect slightly downstream of the top of the first wave. After intersecting, the shock waves continue to propagate and reach the opposite sidewall almost at the location of the wave bottom. The waves are reflected and intersect again around the top of the second wave. Viewed from above, the flow downstream of the first wave crest looks like a succession of lozenges aligned along the channel centreline.

- *Type C* : $Fr^B \leq Fr_1 \leq Fr^C$

For larger Froude numbers, the lateral shock waves intersect at the top of the first wave. At this first intersection, a wave breaking mechanism develops, a small roller appearing on the top of the first wave, immediately downstream of the intersection of the shock waves. The roller has a "cockscorn" shape and is located on the jump centreline. Its size is small compared to the wave (fig. 4). Such a roller is not observed on the second and subsequent waves.

- *Type D* : $Fr^C \leq Fr_1 \leq Fr^D$

At higher Froude numbers, the undular jump features lateral shock waves, a roller and individual air bubble entrainment at the top of the first wave (fig. 4). The bubbles are entrapped at the intersection of the lateral shock waves and the roller and they are entrained over a short distance (less than a single wave length). A small roller might appear at the top of the second wave but no air bubble entrainment is observed there.

- *Type E* : $Fr^D \leq Fr_1 \leq Fr^E$

Just before the disappearance of free-surface undulations downstream of the jump, the roller at the top of the first wave becomes larger and wider. The roller is bounded ("blocked") laterally by the lateral shock waves. A top view of the first wave crest shows a characteristic W-shape formed by the roller on the centreline and the lateral crosswaves (fig. 4). The width of the roller remains smaller than the channel width. A non-negligible air bubble entrainment is observed. The air bubbles can be entrained as far as the second crest.

For upstream Froude numbers larger than the critical value Fr^E , the free-surface undulations downstream of the jump disappear. The jump becomes a weak hydraulic jump and the roller is fully-developed over the entire channel width. In the present study, the disappearance of the undular jump is defined by the disappearance of the second and subsequent wave lengths : i.e., when no energy is radiated

CHANSON, H., and MONTES, J.S. (1995). "Characteristics of Undular Hydraulic Jumps. Experimental Apparatus and Flow Patterns." *Journal of Hydraulic Engineering*, ASCE, Vol. 121, No. 2, pp. 129-144. Discussion : Vol. 123, No. 2, pp. 161-164 (ISSN 0733-9429).

forward in a train of stationary waves. It must be emphasised that even a weak jump might show an initial undulation immediately downstream of the roller. However no subsequent undulations are observed with a weak jump.

For the undular jump types C, D and E, visual observations indicate that the lateral shock waves intersect on the first crest. Subsequent cross-wave intersections do not occur on the wave crests : the length of the shock waves becomes longer than the wave length of the free-surface crests. With increasing Froude numbers, both the wave length and shock-wave length decrease. But the rate of decrease of the wave length is larger than that of the cross-wave length.

The observations obtained during the experiments are summarised in table 2. The transition Froude numbers Fr^A , Fr^B , Fr^C , Fr^D and Fr^E are presented as a function of the aspect ratio y_C/W on figure 5. Previous experimental works are summarised also in table 2.

The present classification applies to undular jumps with upstream fully-developed shear flows. RYABENKO (1990) performed experiments with non-hydrostatic pressure distributions upstream of the jump and proposed another classification. RYABENKO's work suggests that, for upstream flow conditions with non-hydrostatic pressure distribution, the free-surface undulations disappear at lower Froude numbers than for an upstream hydrostatic pressure distribution. HENDERSON (1966) discussed the role of bottom roughness. His photographs suggest that the transition from undular to weak jump occurs at larger Froude numbers for a rough bed than for a smooth bed.

Longitudinal flow pattern

For upstream Froude numbers near unity, the flow pattern downstream of the first crest is two-dimensional (undular jump type A) or symmetrical around the centreline (undular jump type B) down to the downstream gate.

For undular jumps of types C, D and E (i.e. $Fr_1 > Fr^B$), a different free-surface pattern is observed (fig. 6). Immediately downstream of the first crest, the free-surface shows a steady, organised and symmetrical flow pattern. Each wave is clearly marked and maximum wave height is located on the centreline. At the bottom of each wave, the lowest free-surface point is on the centreline. The free-surface at the sidewalls follows the centreline flow pattern (with the same wave length and phase shift) but with much smaller amplitudes. DARCY and BAZIN (1865), FAWER (1937) and HAGER and HUTTER (1984) observed also similar patterns. Note that, for the experiments of FAWER (1937) and HAGER and HUTTER (1984), the channel width was 0.303-m and 0.30-m respectively.

Downstream of the organised flow region, the free-surface develops a chaotic, unsymmetric, unsteady three-dimensional pattern. The wave motion for this disorganised flow pattern shows no visible periodicity in any direction. The free-surface at the sidewalls is subject to large unsteady fluctuations. Some experimental data reported by DARCY and BAZIN (1865, fig. 20) showed the same phenomenon.

Further downstream, a damping flow region exists. The wave amplitudes at the free-surface are damped rapidly over the entire width of the channel, and the free-surface becomes almost quiescent.

CHANSON, H., and MONTES, J.S. (1995). "Characteristics of Undular Hydraulic Jumps. Experimental Apparatus and Flow Patterns." *Journal of Hydraulic Engineering*, ASCE, Vol. 121, No. 2, pp. 129-144. Discussion : Vol. 123, No. 2, pp. 161-164 (ISSN 0733-9429).

Visual observations indicate that the length of the organised flow region decreases with increasing Froude number. Near the disappearance of the undular jump, the length of this region equals one or two wave lengths. For the present study, the number of organised (i.e. coherent) wave lengths N_{OW} is best correlated by :

$$N_{OW} = \left(15.5 + 3.7 \frac{y_c}{W} \right) (Fr^E - Fr_1) \quad \text{for } Fr_1 > Fr^B \quad (6)$$

The authors wish to emphasise that, for a large number of experiments, the damping flow region was clearly observed at the downstream end of the flume. These observations indicate that the chaotic flow region did not result from the reflection of waves by the downstream gate for these experiments. It is believed that the chaotic flow region is a consequence of the interactions between the free-surface undulations and the shock waves when these are not of the same periodicity. In this case, the shock wave propagation disorganises the free-surface undulations and induces three-dimensional wave motion.

Lateral shock waves

When the upstream Froude number equals nearly Fr^A , weak lateral shock waves develop near the sidewalls, these shock waves vanishing when they reach the centre part of the channel (fig. 7). For Froude numbers larger than Fr^A , the shock waves extend over the entire width of the channel and are reflected on the opposite sidewall (fig. 7). The first intersection of the shock waves is always near the top of the first wave crest. MONTES (1986) suggested that the lateral shock waves (or "Mach" waves) are connected with the existence of the sidewall boundary layers. The sidewall boundary layers retard the fluid near the wall and force the apparition of critical condition sooner than on the channel centreline.

In this study, the appearance of crosswaves is independent of the aspect ratio y_c/W and is around $Fr^A = 1.2$ (table 2). IWASA (1955) reported also observations of lateral waves superposed on the free-surface undulations for $Fr_1 \geq 1.5$. FAWER (1937) observed lateral shock waves and he presented a photograph showing crosswaves.

During the experiments, the centreline flow depth h_* at the start of the crosswaves and the angle θ_* between the crosswaves and the sidewalls were recorded. The results indicate that the local Froude number $Fr_* = q_w / \sqrt{g h_*^3}$ and θ_* are independent of the aspect ratio y_c/W and functions of the upstream Froude number only. The start of the oblique jumps occurs in a supercritical flow region such as :

$$Fr_* = Fr_1 - 0.122 \quad (7)$$

The angle of the shock waves and the sidewalls ranges from 20 to 50 degrees, increasing slightly with increasing upstream Froude numbers :

$$\theta_* = 33.32 Fr_1^{0.232} \quad (8)$$

CHANSON, H., and MONTES, J.S. (1995). "Characteristics of Undular Hydraulic Jumps. Experimental Apparatus and Flow Patterns." *Journal of Hydraulic Engineering*, ASCE, Vol. 121, No. 2, pp. 129-144. Discussion : Vol. 123, No. 2, pp. 161-164 (ISSN 0733-9429).

where θ_* is in degrees, and equations (7) and (8) are the best fit of the experimental data. Equation (8) is in opposition with the classical theory of shock waves in supercritical flow (e.g. ROUSE 1938, ENGELUND and MUNCH-PETERESEN 1953) which predicts a reduction in the angle θ_* with increasing Froude numbers.

Experimental data and equation (8) indicate a decrease of the crosswave length with increasing Froude numbers. But the rate of decrease of the length required by the shock waves to cross the flume is much smaller than the rate of decrease of the free-surface wave length.

The lateral shock waves are a main feature of the undular jump. They appear in a region of positive pressure gradient (i.e. $dP/dx > 0$) where the modification of the vertical velocity and pressure distributions interacts with the lateral (sidewall) boundary layers. The authors believe that the lateral shock waves result from these interactions. In essence, the wall boundary layer is subjected to a sudden adverse pressure gradient which causes a sharp deceleration of the velocity near the wall and possibly separation. Indeed, a recirculation of the flow indicating separation is observed immediately behind the lateral shock waves near the wall. This is commented upon in the next section. In any case, the complete process is not yet fully understood.

Flow recirculation

Dye injections were used to observe recirculations or separation bubbles, at various locations along undular jumps near the bottom or along the sidewalls. Two types of recirculation are visualised : a free-surface recirculation at the first crest and a corner recirculation at the location of the first crest and sometimes at the location of subsequent crests (fig. 8).

Immediately after the apparition of the lateral shock waves (i.e. $Fr_1 > Fr^A$), and at the first crest only (fig. 8), countercurrents are clearly observed near the free surface between the developing shock waves and the sidewalls (fig. 8). A large-scale vortex of quasi-vertical axis develops along each sidewall next to the free-surface and immediately upstream of the first crest. Visual observations suggest that the strength of the recirculatory motion increases with increasing Froude number for $Fr_1 > Fr^A$.

For larger Froude numbers, another form of recirculation becomes apparent near the corners formed by the channel bottom and the sidewalls (fig. 8). This corner recirculation is located at the first wave crest cross-section and at the second and successive crest positions for increasing Froude numbers (table 3). Such a recirculation is not observed elsewhere. At the first wave crest, the corner recirculating motion does not interact with the free-surface recirculation. It is thought that this recirculatory motion is generated by the interactions between the expanding flow motion immediately upstream of the wave crest, the sidewall boundary layers and the bottom boundary layer.

FAWER (1937), MONTES (1986) and YASUDA et al. (1993) observed a separation bubble on the bottom centreline of the channel below the first crest. In their experiments, the undular jump was located immediately downstream of a sluice gate and the upstream flow was partially developed. During the present series of experiments, dye injection indicated no recirculation or separation bubble on the centreline next to the channel bottom.

CHANSON, H., and MONTES, J.S. (1995). "Characteristics of Undular Hydraulic Jumps. Experimental Apparatus and Flow Patterns." *Journal of Hydraulic Engineering*, ASCE, Vol. 121, No. 2, pp. 129-144. Discussion : Vol. 123, No. 2, pp. 161-164 (ISSN 0733-9429).

EXPERIMENTAL RESULTS

Free-surface profiles

For discharges per unit width ranging from 0.008 to 0.12 m²/s and upstream Froude numbers between 1.05 and 3.0, the free-surface profiles on the centreline were recorded upstream and downstream of the jump. The complete set of data were reported in CHANSON (1993).

Figures 9 and 10 present the dimensionless wave lengths and wave amplitudes (on the channel centreline) as functions of the upstream Froude number. The data are compared with the solution of the Boussinesq equation developed by ANDERSEN (1978).

Wave length

For small Froude numbers, the measured wave lengths are close to the solution of the Boussinesq equation (fig. 9). For larger Froude numbers, the relationship between the dimensionless wave length and the Froude number is no longer unique but depends upon the ratio of the critical depth over the channel width : i.e., for a given Froude number, the wave length increases with a decrease of the aspect ratio y_c/W .

One possible explanation is related to the appearance of the lateral shock waves on the surface. The authors believe that the shock waves affect the wave length and induce a dependence of the wave length upon the channel width when the free-surface wave length becomes shorter than the distance along the channel necessary for the shock waves to cross the channel (i.e. $Fr_1 > Fr^B$).

It is worth noting that, for constant Froude number, a decrease of discharge (and of blockage ratio) gives an increase in dimensionless wave length (fig. 9). Note also that, for constant Froude number, a decrease in discharge implies an increase of relative roughness and of channel friction. This result is opposite to the findings for ZIENKIEWICZ and SANDOVER (1957) who studied undular surges and found that the channel friction reduced the wave length. It is thought that the analogy between undular surge and undular jump cannot be applied to this situation.

Figure 11 shows the dimensionless wave length as a function of the wave length number : the i -th wave length is measured between the i -th wave crest and the $(i+1)$ -th crest. The analysis of all data indicates clearly that the wave lengths decay exponentially along the channel (fig. 11). Further it shows that the rate of decay is independent of the upstream Froude number, of the aspect ratio and of the type of undular jump. For the experiments, the wave length decay can be correlated by :

$$\frac{L_{wi}}{L_{w1}} = (i)^{-1/5} \quad (9)$$

where L_{w1} is the first wave length and i is the wave length number (fig. 11).

CHANSON, H., and MONTES, J.S. (1995). "Characteristics of Undular Hydraulic Jumps. Experimental Apparatus and Flow Patterns." *Journal of Hydraulic Engineering*, ASCE, Vol. 121, No. 2, pp. 129-144. Discussion : Vol. 123, No. 2, pp. 161-164 (ISSN 0733-9429).

Wave amplitude

Figure 10 shows that the relationship between the dimensionless wave amplitude and the upstream Froude number has a distinctive shape. The shape is generalised in figure 12 and can be described as follow :

- 1- For Froude numbers close to unity, the data follow closely the theoretical solution of the Boussinesq equation (ANDERSEN 1978). The wave amplitude is almost proportional to the Froude number (i.e. $\Delta h/y_c \propto (Fr_1 - 1)$).
- 2- With increasing Froude number, the wave amplitude data start diverging from the solution of the motion equation (i.e. this equation neglecting energy dissipation considerations) and reach a maximum value $(\Delta h)_{max}$. This trend is consistent with the data presented by both IWASA (1955) and MONTES (1979), and with a re-analysis of the data of BINNIE and ORKNEY (1955).
- 3- For larger Froude numbers, the wave amplitude decreases with increasing Froude number.
- 4- Before the disappearance of the free-surface undulations, the wave amplitude stops decreasing with increasing Fr_1 . At the limit, when the undular jump tends to become a weak jump, the amplitude of the first wave will tend to a value equal to half of the roller height, and the amplitude of the second wave will tend to zero (fig. 10).

Figure 10 shows distinctly that both the divergence of the data with the Boussinesq equation solution and the maximum dimensionless undulation amplitude are functions of the aspect ratio. For these experiments, the experimental data of the maximum wave amplitude $(\Delta h)_{max}$ and the corresponding upstream Froude number Fr^m (fig. 12) can be correlated by:

$$\frac{(\Delta h)_{max}}{y_c} = 0.0748 \left(\frac{y_c}{W} \right)^{-0.894} \quad (10)$$

$$Fr^m = 1.02 \left(\frac{y_c}{W} \right)^{-0.247} \quad (11)$$

Equations (10) and (11) were obtained for $0.137 < y_c/W < 0.454$.

Note that the Froude number Fr^m equals approximately the Froude number Fr^B characterising the appearance of a "cockscorn" roller on the first wave crest (table 2, columns 4 and 5). It is believed that the wave breaking mechanism, associated with the small roller, contributes to the reduction of the wave amplitude.

FAWER (1937) was able to set up undular jumps at variable distances downstream of a gate. He noted that the undulations were steeper and more two-dimensional when the jump was close to the gate : i.e., when the upstream boundary layer was thin ($\delta/h_1 \ll 1$), where δ is the boundary layer thickness.

Visual observations and measurements show that the longitudinal decay of the wave amplitude is very small and sometimes zero, while a decay of the wave lengths along the flume is consistently observed for all the experiments. DARCY and BAZIN (1865) established an undular jump at the end of 75-m long channel, the upstream flow conditions of the jump being fully-developed. A re-analysis of their data indicates

CHANSON, H., and MONTES, J.S. (1995). "Characteristics of Undular Hydraulic Jumps. Experimental Apparatus and Flow Patterns." *Journal of Hydraulic Engineering*, ASCE, Vol. 121, No. 2, pp. 129-144. Discussion : Vol. 123, No. 2, pp. 161-164 (ISSN 0733-9429).

similarly no decay of the wave amplitude along the channel. With regard to partially developed upstream shear flows, FAWER (1937) reported that the wave amplitude did not decay along the 5-m long channel.

Velocity, pressure and specific energy distributions on the centreline

For various Froude numbers and discharges, measurements of centreline velocity, pressure and total head distributions were performed at various locations along the undular jump : i.e., upstream of the jump (U/S), at the start of the lateral shock waves (SW), at the first crest (1C) and first bottom (1B), at the second crest (2C) and second bottom (2B), at the third crest(3C). The complete set of data was presented in CHANSON (1993).

Figure 13 presents a typical set of experimental data obtained along the channel centreline. The pressure distributions (fig. 13A) are presented as $P/(\rho_w g h)_{CL}$ versus y/h where P is the pressure and h is the centreline flow depth. On figure 13B, the dimensionless velocity $V/(V_m)_{CL}$ is plotted as a function of y/h , where V is the local velocity and $(V_m)_{CL}$ is the mean centreline velocity :

$$(V_m)_{CL} = \left(\frac{1}{h} \int_{y=0}^{y=h} V dy \right)_{CL} \quad (12)$$

Figure 13C show the dimensionless specific energy $E/(E_m)_{CL}$ as a function of y/h . The local specific energy E is the energy per unit weight and gravity unit with the elevation datum being taken as the bottom of the channel (CHOW 1959) :

$$E = \frac{P}{\rho_w g} + y \cos \alpha + \frac{V^2}{2g} \quad (13)$$

where α is the channel slope, and the mean specific energy on the centreline $(E_m)_{CL}$ being defined as :

$$(E_m)_{CL} = \left(\frac{\int_{y=0}^{y=h} E V dy}{\int_{y=0}^{y=h} V dy} \right)_{CL} \quad (14)$$

Figure 13A provides a comparison between the pressure distributions along the jump and the upstream hydrostatic pressure distribution (U/S Ref.). On figure 13B, the velocity distributions can be compared with the upstream power law velocity distribution (eq. (4)).

DISCUSSION : EFFECTS OF THE ASPECT RATIO

For open channel flows, the Froude number equals the ratio of the mean flow velocity over the celerity of small disturbances, and is analogous to the Mach number for compressible flows. As the Mach number for compressible flows, the Froude number is the most important correlating parameter when flow depths are

CHANSON, H., and MONTES, J.S. (1995). "Characteristics of Undular Hydraulic Jumps. Experimental Apparatus and Flow Patterns." *Journal of Hydraulic Engineering*, ASCE, Vol. 121, No. 2, pp. 129-144. Discussion : Vol. 123, No. 2, pp. 161-164 (ISSN 0733-9429).

almost critical flow depths : i.e., when the mean specific energy is near its minimum value. In a undular jump, critical flow occurs somewhere between the upstream flow cross-section and the first wave crest. At that location (i.e. $h = y_c$), the sidewalls induce a blockage effect that can be best described by the aspect ratio y_c/W . For a wide channel (i.e two-dimensional flow), the aspect ratio is zero and the sidewalls have no effect on the flow. For a narrow channel (i.e. y_c/W large), the sidewalls induce significant three-dimensional effects.

All the present experiments have been performed with a constant channel width and various flow rates. Additional flow visualisations were conducted in a wider channel at the University of Tasmania. Also previous experiments were conducted by several authors with various channel widths ranging from 0.2 to 1 m (table 1).

A re-analysis of all data (i.e. $W = 0.2$ to 1 m) indicates, in each case, a similar dependence of the flow characteristics upon the critical depth y_c . The relationship wave amplitude-Froude number (fig. 10 and 12) exhibits the same features for all experiments. Furthermore a comparison of all experimental results in term of y_c/W shows that, for constant Froude number, the dimensionless wave length L_w/y_c and amplitude $\Delta h/y_c$ increase with decreasing aspect ratio y_c/W (fig. 9 and 10). Also the upper limit of undular jump Fr^E decreases with increasing y_c/W for fully-developed upstream flow conditions (table 2 and fig. 5).

The authors believe that the blockage ratio y_c/W is a major parameter but not the only one characterising the undular jump. RYABENKO (1990) and CHANSON (1993) showed that the upstream flow conditions (i.e. partially-developed or fully-developed boundary layer flow) affect strongly the flow characteristics. Furthermore the characteristics of the sidewall boundary layers are important parameters. For fully-developed upstream flows, the authors are convinced that the relative roughness of the sidewall $(k_s)_{wall}/(W/2)$, and hence the channel width, may be a significant parameter. At the present time, there is no quantitative information on the dependence of the flow characteristics upon these variables.

CONCLUSION

New undular hydraulic jump experiments were performed in a long tilting flume of rectangular cross-section. The upstream flows were fully-developed shear flows.

Visual and photographic investigations indicate five (5) different types of undular jumps, the main flow patterns of which are completely different from undular surge flows. The present study shows that the shape of the jump and its main flow characteristics are strongly correlated to the upstream Froude number and to the aspect ratio y_c/W .

One characteristic feature of undular jumps is the presence of lateral shock waves for Froude numbers larger than 1.2. The shock waves start in a region of supercritical flow and intersect at the first wave crest. The angle θ^* between the shock waves and the sidewalls increases with increasing Froude number. Such a result contradicts the theory of shock waves and is not explained yet.

CHANSON, H., and MONTES, J.S. (1995). "Characteristics of Undular Hydraulic Jumps. Experimental Apparatus and Flow Patterns." *Journal of Hydraulic Engineering*, ASCE, Vol. 121, No. 2, pp. 129-144. Discussion : Vol. 123, No. 2, pp. 161-164 (ISSN 0733-9429).

Free-surface profiles were recorded for a wide range of discharge and Froude number. For small Froude numbers, the first wave length and the wave amplitude can be estimated by undular surge theory calculations. But for increasing Froude numbers, both the first wave length and amplitude become dependent upon the aspect ratio : i.e. for a given Froude number, the dimensionless first wave length and amplitude increase with decreasing ratio y_c/W . Other results of this series of experiments show : wave amplitudes as large as $(0.47 y_c)$; the disappearance of the undular jump for upstream Froude numbers ranging from 1.5 up to 2.9; an exponential decay of the wave length along an undular jump; and a small or zero decay of the wave amplitude along the jump.

This work emphasises the three-dimensional flow characteristics of undular jumps with fully-developed upstream flows in a rectangular channel. Further work is required in the form of three-dimensional measurements of both free-surface level and also velocity, pressure and total head distributions along these jumps. Additional work is necessary to understand the mechanisms of lateral shock waves.

APPENDIX I. REFERENCES

- ANDERSEN, V.M. (1978). "Undular Hydraulic Jump." *Jl of Hyd. Div.*, ASCE, Vol. 104, No. HY8, pp. 1185-1188.
- BAKHMETEFF, B.A., and MATZKE, A.E. (1936). "The Hydraulic Jump in Terms of Dynamic Similarity." *Transactions*, ASCE, Vol. 101, pp. 630-647. Discussion : Vol. 101, pp. 648-680.
- BINNIE, A.M., and ORKNEY, J.C. (1955). "Experiments on the Flow of Water from a Reservoir through an Open Channel. II. The Formation of Hydraulic Jump." *Proc. Royal Soc., London, Series A*, Vol. 230, pp. 237-245.
- CHANDRAN, K.K., and VENKATRAMAN, C.P. (1985). "Hydraulic Design of Pump Intake for Cooling Water Pumps Parli Thermal Power Station (Unit IV), Maharashtra, India." *Proc. Intl Conf. Hydraulics of Pumping Stations*, BHRA, Manchester, UK, paper 11, pp. 139-148.
- CHANSON, H. (1993). "Characteristics of Undular Hydraulic Jumps." *Research Report No. CE146*, Dept. of Civil Engineering, University of Queensland, Australia Nov., 109 pages.
- CHEN, C.L. (1990). "Unified Theory on Power Laws for Flow Resistance." *Jl of Hyd. Engrg.*, ASCE, Vol. 117, No. 3, pp. 371-389.
- CHOW, V.T. (1959). "Open Channel Hydraulics." *McGraw-Hill International*, New York, USA.
- DARCY, H., and BAZIN, H. (1865). "Recherches Hydrauliques." *Imprimerie Impériales*, Parties 1e et 2e, Paris, France (in French).
- ENGELUND, F., and MUNCH-PETERSEN, J. (1953). "Steady Flow in Contracted and Expanded Rectangular Channels. Some Considerations Concerning the Shape of the Water Surface." *Jl La Houille Blanche*, Aug./Sept., pp. 464-474.

- CHANSON, H., and MONTES, J.S. (1995). "Characteristics of Undular Hydraulic Jumps. Experimental Apparatus and Flow Patterns." *Journal of Hydraulic Engineering*, ASCE, Vol. 121, No. 2, pp. 129-144. Discussion : Vol. 123, No. 2, pp. 161-164 (ISSN 0733-9429).
- FAWER, C. (1937). "Etude de Quelques Ecoulements Permanents à Filets Courbes." ('Study of some Steady Flows with Curved Streamlines.') *Thesis*, Lausanne, Switzerland, Imprimerie La Concorde, 127 pages (in French).
- HAGER, W.H., and HUTTER, K. (1984). "On Pseudo-Uniform Flow in Open Channel Hydraulics." *Acta Mechanica*, Vol. 53, pp. 183-200.
- HASLEWOOD, D. (1985). "Ships in Restricted Waters (Critical Conditions)." *Proc. Instn Civ. Engrs*, Part 2, Vol. 79, June, pp. 275-293.
- HENDERSON, F.M. (1966). "Open Channel Flow." *MacMillan Company*, New York, USA.
- ISAACS, L.T., and MACINTOSH, J.C. (1988). "Boundary Shear Stress Measurement in Open Channels." *Research Report No. CE85*, Dept. of Civil Eng., Univ. of Queensland, Brisbane, Australia, 57 pages.
- IWASA, Y. (1955). "Undular Jump and its Limiting Conditions for Existence." *Proc. of the 5th Japan National Congress for Applied Mechanics*, Paper II-14, pp. 315-319.
- JONES, L.E. (1964). "Some Observations on the Undular Jump." *Jl of Hyd. Div.*, ASCE, Vol. 90, No. HY3, pp. 69-82.
- LEMOINE, R. (1948). "Sur les Ondes Positives de Translation dans les Canaux et sur le Ressaut Ondulé de Faible Amplitude." *Jl La Houille Blanche*, Mar-Apr., pp. 183-185 (in French).
- MONTES, J.S. (1979). "Undular Hydraulic Jump - Discussion." *Jl of Hyd. Div.*, ASCE, Vol. 105, No. HY9, pp. 1208-1211.
- MONTES, J.S. (1986). "A Study of the Undular Jump Profile." *Proc. of the 9th Australasian Fluid Mechanics Conference AFMC*, Auckland, New Zealand, pp. 148-151.
- OVALLE, A., and DOMINGUEZ, A. (1934). *Civil Engineering Thesis*, Catholic University, Santiago, Chile.
- ROUSE, H. (1938). "Fluid Mechanics for Hydraulic Engineers." *McGraw-Hill*, New York, USA.
- RYABENKO, A.A. (1990). "Conditions Favorable to the Existence of an Undulating Jump." *Gidrotekhnicheskoe Stroitel'stvo*, No. 12, pp. 29-34 (in Russian). (Translated in *Hydrotechnical Construction*, 1990, Plenum Publ., pp. 762-770).
- SANDOVER, J.A., and HOLMES, P. (1962). "The Hydraulic Jump in Trapezoidal Channels." *Water Power*, Nov., pp. 445-449.
- SERRE, F. (1953). "Contribution à l'Etude des Ecoulements Permanents et Variables dans les Canaux." *Jl La Houille Blanche*, Dec., pp. 830-872 (in French).
- STREETER, V.L., and WYLIE, E.B. (1981). "Fluid Mechanics." *McGraw-Hill*, 1st SI Metric edition, Singapore.
- YASUDA, Y., OHTSU, I., and GOTOH, H. (1993). "A Few Experiments on Undular Hydraulic Jump." *48th Annual Meeting JSCE*, Japan, Sept., p. II-159 (in Japanese).
- ZIENKIEWICZ, O.C., and SANDOVER, J.A. (1957). "The Undular Surge Wave." *Proc. 7th IAHR Congress*, Vol. II, Lisbon, Portugal, paper D25, pp. D1-11.

CHANSON, H., and MONTES, J.S. (1995). "Characteristics of Undular Hydraulic Jumps. Experimental Apparatus and Flow Patterns." *Journal of Hydraulic Engineering*, ASCE, Vol. 121, No. 2, pp. 129-144. Discussion : Vol. 123, No. 2, pp. 161-164 (ISSN 0733-9429).

APPENDIX II. NOTATION.

The following symbols are used in this paper :

- h = flow depth (m) measured perpendicular to the channel bottom;
- y_c = critical flow depth (m) : for a rectangular channel : $y_c = \sqrt[3]{q_w^2/g}$;
- h_* = centreline flow depth (m) at the start of the lateral shock waves;
- E = specific energy (m);
- $(E_m)_{CL}$ = mean specific energy (m) on the centreline;
- Fr = Froude number defined as : $Fr = q_w/\sqrt{g h^3}$;
- Fr^A = Froude number characterising the apparition of lateral shock waves;
- Fr^B = Froude number characterising the apparition of a small "cockscomb" roller at the top of the first wave crest;
- Fr^C = Froude number characterising the apparition of individual air bubble entrainment;
- Fr^D = Froude number characterising the apparition of a roller formed in between the lateral shock waves and a substantial air entrainment;
- Fr^E = Froude number characterising the disappearance of the undular jump;
- Fr^m = upstream Froude number corresponding to the maximum wave amplitude;
- Fr^{RFS} = Froude number characterising the onset of free-surface recirculation at the first crest;
- Fr^{R1C} = Froude number characterising the onset of corner recirculation at the first crest;
- Fr^{R2C} = Froude number characterising the onset of corner recirculation at the second crest;
- Fr^{R3C} = Froude number characterising the onset of corner recirculation at the third crest;
- Fr* = Froude number defined in term of the centreline flow depth at the inception of the lateral shock waves : $Fr_* = q_w/\sqrt{g h_*^3}$;
- f = Darcy friction factor;
- g = gravity constant : $g = 9.80 \text{ m/s}^2$ in Brisbane, Australia;
- H = total head (m);
- i = wave length number;
- K = Von Karman constant;
- k = constant of proportionality;
- k_s = equivalent sand roughness height (m);
- L_w = wave length (m);
- N = exponent of the power law velocity distribution;
- N_{ow} = number of organised wave lengths;
- P = pressure (Pa);
- Q_w = water discharge (m^3/s);

CHANSON, H., and MONTES, J.S. (1995). "Characteristics of Undular Hydraulic Jumps. Experimental Apparatus and Flow Patterns." *Journal of Hydraulic Engineering*, ASCE, Vol. 121, No. 2, pp. 129-144. Discussion : Vol. 123, No. 2, pp. 161-164 (ISSN 0733-9429).

q_w = water discharge per unit width (m^2/s);

V = velocity (m/s);

V_c = critical flow velocity (m/s) : $V_c = q_w/y_c$;

V_{max} = maximum velocity on the centreline (m/s) (at the free-surface);

$(V_m)_{CL}$ = mean velocity on the centreline (m/s);

W = channel width (m);

x = distance along the channel bottom (m);

y = distance measured perpendicular to the channel bottom (m);

z = bed elevation (m) taken positive upward;

α = channel slope;

Δh = wave amplitude (m);

$(\Delta h)_{max}$ = maximum wave amplitude (m);

ΔH = head loss (m);

δ = boundary layer thickness (m);

θ_* = angle between the lateral shock waves and the sidewalls at the start of the lateral shock waves;

ρ_w = water density (kg/m^3);

\varnothing = diameter (m);

Subscript

CL = on the flume centreline;

i = wave length number;

1 = flow conditions upstream of the hydraulic jump;

2 = flow conditions downstream of the hydraulic jump;

CHANSON, H., and MONTES, J.S. (1995). "Characteristics of Undular Hydraulic Jumps. Experimental Apparatus and Flow Patterns." *Journal of Hydraulic Engineering*, ASCE, Vol. 121, No. 2, pp. 129-144. Discussion : Vol. 123, No. 2, pp. 161-164 (ISSN 0733-9429).

Table 1. Summary of experimental flow conditions

Reference (1)	q_w m^2/s (2)	h_1 m (3)	Fr_1 (4)	y_c/W (5)	U/S Flow (6)	Nb of Exp. (7)	Comments (8)
<u>Present study</u>							
University of Queensland	0.008	0.010 to 0.017	1.13 to 2.6	0.075	F/D	6	Series HMUP1. W = 0.25 m.
	0.020	0.016 to 0.032	1.14 to 2.91	0.137	F/D	18	Series HMUP2.
	0.028	0.029 to 0.041	1.08 to 1.79	0.172	F/D	8	Series HC3.
	0.040	0.027 to 0.051	1.11 to 2.83	0.219	F/D	19	Series HMUP3.
	0.042	0.037 to 0.051	1.10 to 1.77	0.224	F/D	9	Series HC1.
	0.062	0.061	1.31	0.292	F/D	1	Series HC0.
	0.08	0.067 to 0.084	1.05 to 1.49	0.347	F/D	7	Series HC4.
	0.12	0.091 to 0.109	1.07 to 1.40	0.454	F/D	6	Series HC2.
University of Tasmania			1.1 to 10		P/D		W = 0.4 m.
ANDERSEN (1978)	0.066	0.067	1.22	N/A	N/A	1	
BAKHMETEFF and MATZKE (1936)	0.327	0.135 to 0.155	1.75 to 2.1	1.45	P/D	3	W = 0.152 m.
FAWER (1937)	0.02 to 0.07	0.02 to 0.08	1.3 to 1.75	0.11 to 0.27	P/D	5	W = 0.303 m.
BINNIE and ORKNEY (1955)	0.069 to 0.084	0.064	1.12 to 1.52	N/A	P/D	6	
DARCY and BAZIN (1865)	1.55 (?)	0.43	1.76 (?)	N/A	F/D	1	Aqueduc of Crau, canal of Craponne (France).
HAGER and HUTTER (1984)	0.0987	0.081	1.37	0.332	P/D	1	W = 0.3 m. $\alpha = 0.08$ deg.
IWASA (1955)	N/A	N/A	1.29 to 4.14	N/A	N/A	34	
MONTES (1979)	N/A	N/A	1.25 to 2	N/A	P/D	8	W = 0.2 m.
YASUDA et al. (1993)	0.025 to 0.085	0.023 to 0.067	1.5 to 2.17	0.101 to 0.208	F/D & P/D	4	W = 0.3 to 0.4 m. Horizontal channel.
RYABENKO (1990)	0.025 to 0.38	0.03 to 0.2	1 to 4.0	0.04 to 0.25	F/D & P/D	13	W = 1m.

Notes :

Nb. of Exp. : number of experiments

U/S Flow : upstream flow conditions :

(F/D) : fully developed boundary layer flow (i.e. $\delta = h_1$);

P/D : partially developed boundary layer flow (i.e. $\delta/h_1 < 1$);

N/A : not available.

CHANSON, H., and MONTES, J.S. (1995). "Characteristics of Undular Hydraulic Jumps. Experimental Apparatus and Flow Patterns." *Journal of Hydraulic Engineering*, ASCE, Vol. 121, No. 2, pp. 129-144. Discussion : Vol. 123, No. 2, pp. 161-164 (ISSN 0733-9429).

Table 2. Characteristic Froude numbers

Reference (1)	y_c/W (2)	Fr^A (3)	Fr^B (4)	Fr^m (5)	Fr^C (6)	Fr^D (7)	Fr^E (8)	Remarks (9)	
<u>Present work</u>	0.075	1.22	1.72		2.10	2.40	> 2.6	Series HMUP1.	
	0.137	1.22	1.68	1.68	1.80	2.4	2.91	Series HMUP2.	
	0.172	1.2	1.45	1.58	1.7			Series HC3.	
	0.219	1.26	1.33	1.51	1.65	2.2	2.83	Series HMUP3.	
	0.224			1.47	1.65			Series HC1.	
	0.347	1.10	1.18	1.27	1.4	1.49	1.6	Series HC4.	
	0.454	1.2	1.25	1.27	1.35		1.5	Series HC2.	
OVALLE and DOMINGUEZ (1934) ^(a)							1.59		
							3.63	With special precautions.	
BAKHMETEFF and MATZKE (1936) ^(b)							2.1	W = 0.152 m.	
FAWER (1937)	0.1 to 0.27				1.82		2.46	W = 0.303 m.	
SERRE (1953)								1.455	Theory.
BINNIE and ORKNEY (1955)								1.74	
IWASA (1955)						1.5		1.9	
							1.553	Theory.	
RYABENKO (1990)	0.090							2.08	Hydrostatic
	0.143							1.90	pressure
	0.147							1.95	distribution
	0.185							1.82	upstream of the
	0.187							1.86	jump (W = 1 m).
	0.192							1.92	
	0.224							1.69	
	0.231							1.77	
	0.239							1.88	
	0.244							1.94	
	0.060							1.01	Non-hydrostatic
	0.109							1.34	pressure
	0.121							1.02	distribution
	0.010							1.0	upstream of the
0.041							1.03	jump (W = 1 m).	
0.043							1.25		
0.044							1.42		
0.124							1.61		

Notes :

(a) : as cited by MONTES (1986).

(b) : BAKHMETEFF and MATZKE (1936) indicate an upper limit for undular jumps of $Fr_1 = 1.732$.

A re-analysis of their data indicate that the upper limit for their experiments was $Fr_1 = 2.1$.

Table 3 - Onset of recirculation

Froude number (1)	y_c/W		Comments (4)
	0.138 (2)	0.217 (3)	
Fr_{RFS}	1.25	1.26	Apparition of free-surface recirculation.
Fr_{R1C}	1.41	1.35	Apparition of corner recirculation at the first wave crest.
Fr_{R2C}	1.50	1.47	Apparition of corner recirculation at the second wave crest.
Fr_{R3C}	1.64	1.52	Apparition of corner recirculation at the third wave crest.

CHANSON, H., and MONTES, J.S. (1995). "Characteristics of Undular Hydraulic Jumps. Experimental Apparatus and Flow Patterns." *Journal of Hydraulic Engineering*, ASCE, Vol. 121, No. 2, pp. 129-144. Discussion : Vol. 123, No. 2, pp. 161-164 (ISSN 0733-9429).

Fig. 1 - Sketch of an undular hydraulic jump

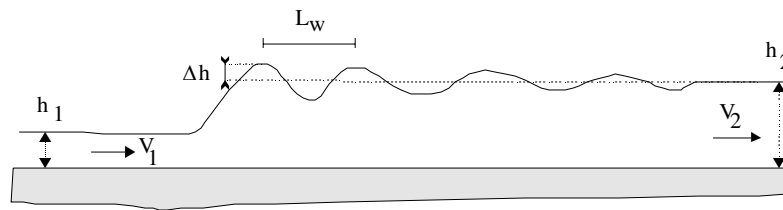


Fig. 2 - Photograph of the experiment - $y_c/W = 0.138$, $Fr_1 = 1.62$, $W = 0.25$ m (UJ type C)
Flow from the right to the left

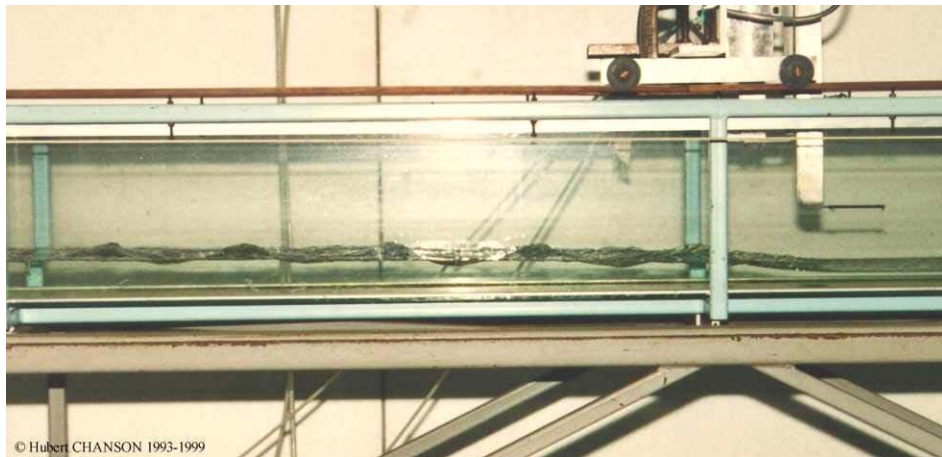
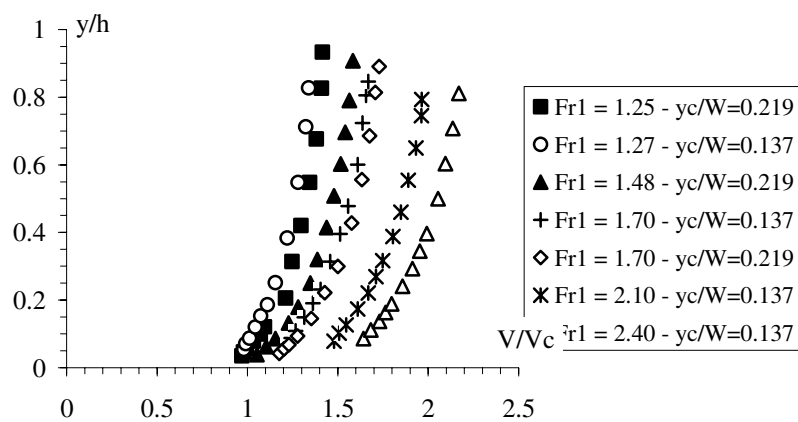
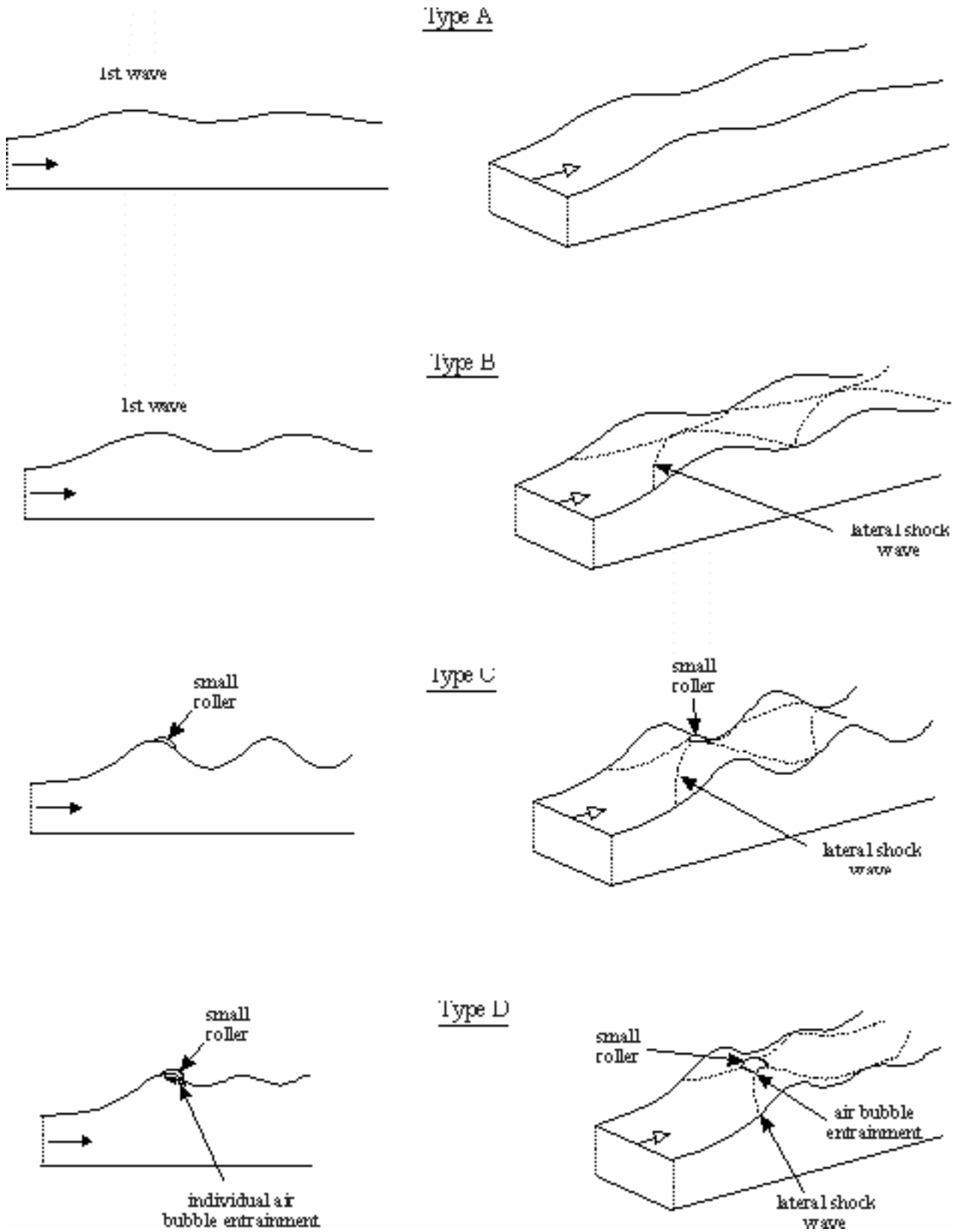


Fig. 3 - Typical velocity distributions upstream of the undular jump



CHANSON, H., and MONTES, J.S. (1995). "Characteristics of Undular Hydraulic Jumps. Experimental Apparatus and Flow Patterns." *Journal of Hydraulic Engineering*, ASCE, Vol. 121, No. 2, pp. 129-144. Discussion : Vol. 123, No. 2, pp. 161-164 (ISSN 0733-9429).

Fig. 4 - Classification of undular hydraulic jumps



CHANSON, H., and MONTES, J.S. (1995). "Characteristics of Undular Hydraulic Jumps. Experimental Apparatus and Flow Patterns." *Journal of Hydraulic Engineering*, ASCE, Vol. 121, No. 2, pp. 129-144. Discussion : Vol. 123, No. 2, pp. 161-164 (ISSN 0733-9429).

Fig. 4 - Classification of undular hydraulic jumps

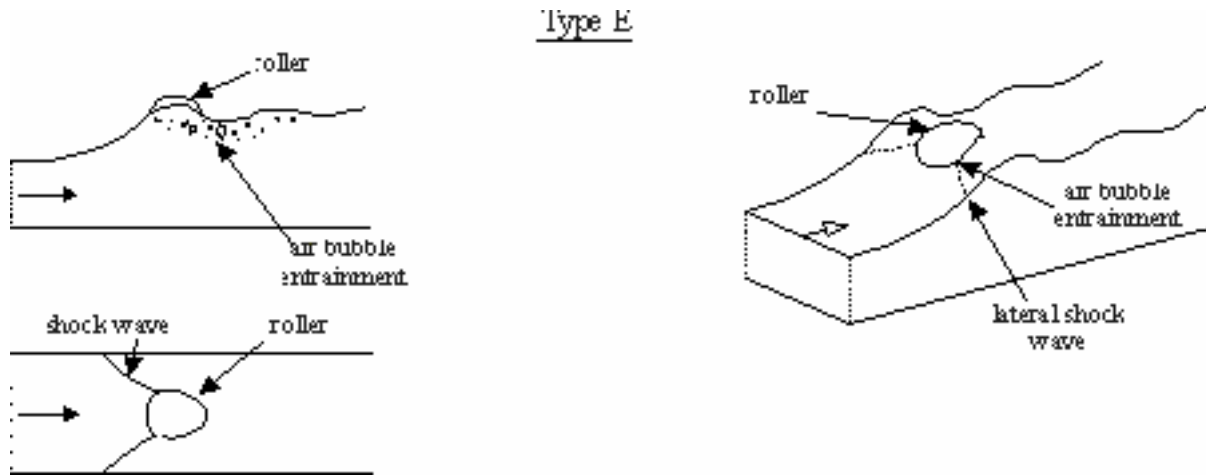
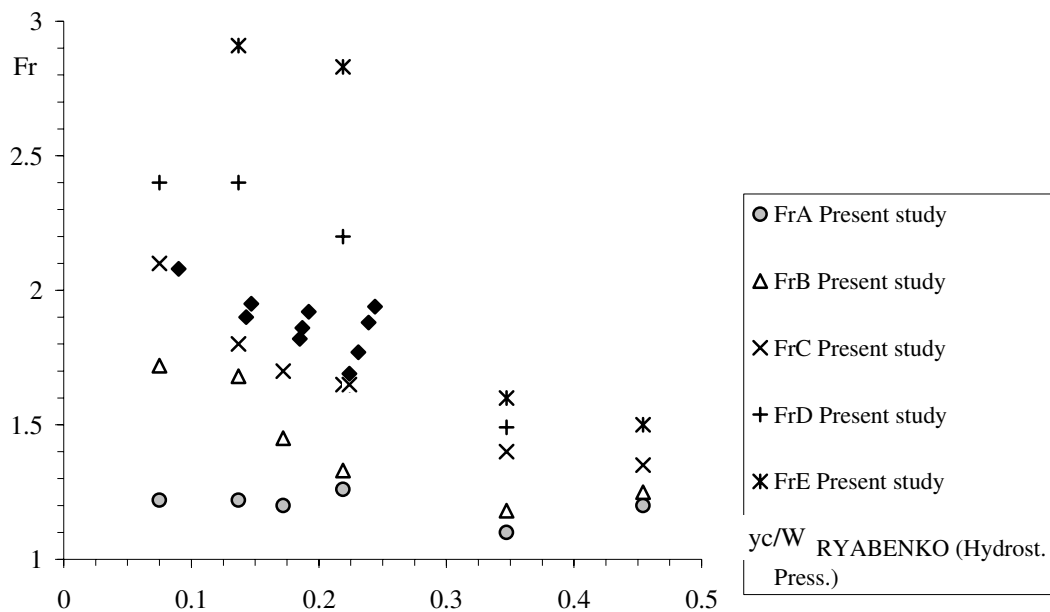


Fig. 5 - Characteristic Froude numbers as a function of the aspect ratio y_c/W

Present study and RYABENKO (1990)



CHANSON, H., and MONTES, J.S. (1995). "Characteristics of Undular Hydraulic Jumps. Experimental Apparatus and Flow Patterns." *Journal of Hydraulic Engineering*, ASCE, Vol. 121, No. 2, pp. 129-144. Discussion : Vol. 123, No. 2, pp. 161-164 (ISSN 0733-9429).

Fig. 6 - Flow regions downstream of the first crest: organised flow region, chaotic flow region and damping flow region

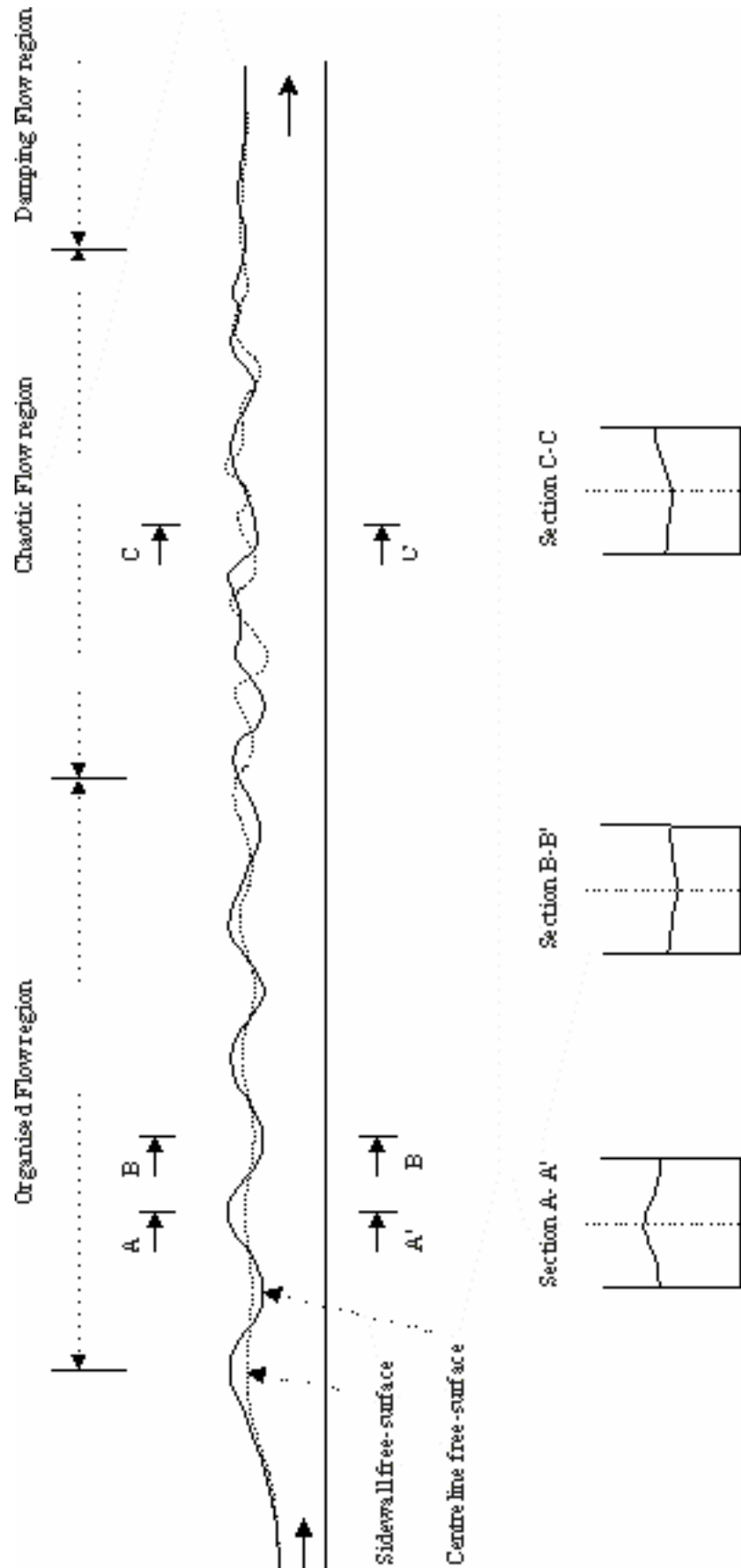
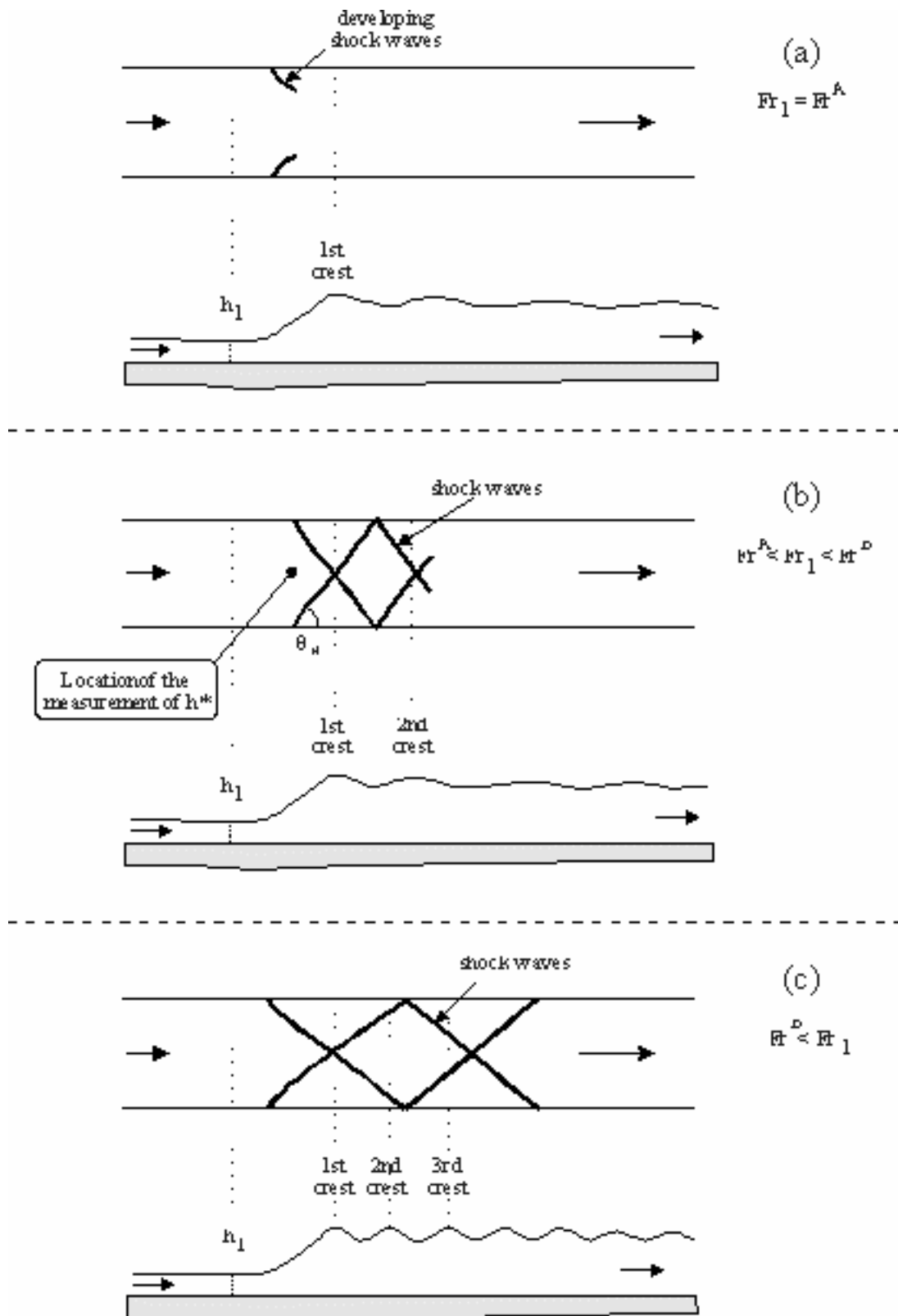


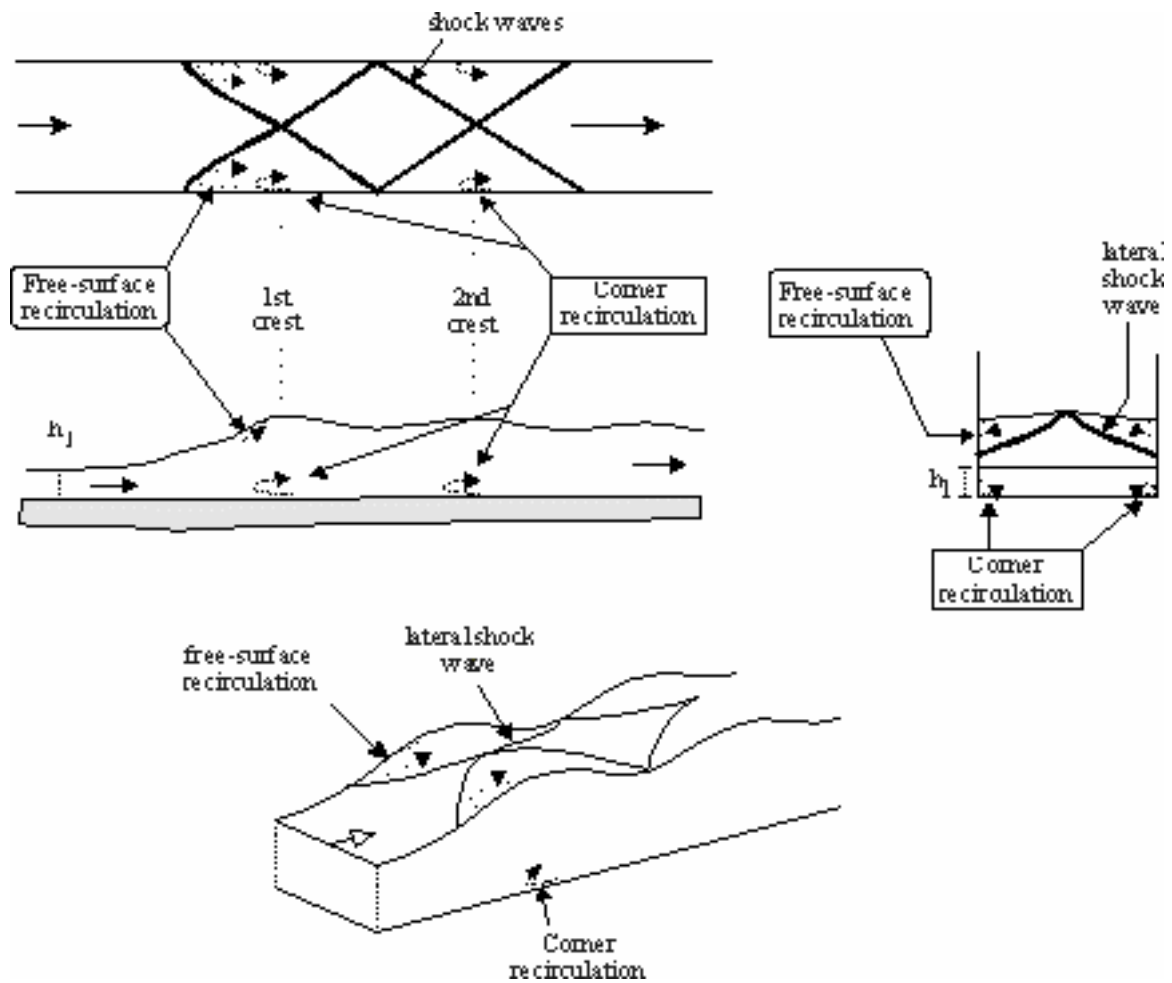
Fig. 7 - Sketch of lateral shock waves (top view) :

(a) $Fr_1 = Fr^A$; (b) $Fr^A < Fr_1 < Fr^B$; (c) $Fr^B < Fr_1$



CHANSON, H., and MONTES, J.S. (1995). "Characteristics of Undular Hydraulic Jumps. Experimental Apparatus and Flow Patterns." *Journal of Hydraulic Engineering*, ASCE, Vol. 121, No. 2, pp. 129-144. Discussion : Vol. 123, No. 2, pp. 161-164 (ISSN 0733-9429).

Fig. 8 - Recirculatory flow motion near the free-surface and in the corners
(shock waves drawn for a Type-C jump)



CHANSON, H., and MONTES, J.S. (1995). "Characteristics of Undular Hydraulic Jumps. Experimental Apparatus and Flow Patterns." *Journal of Hydraulic Engineering*, ASCE, Vol. 121, No. 2, pp. 129-144. Discussion : Vol. 123, No. 2, pp. 161-164 (ISSN 0733-9429).

Fig. 9 - Dimensionless wave length L_w/y_c as a function of the upstream Froude number Fr_1 (First wavelength)

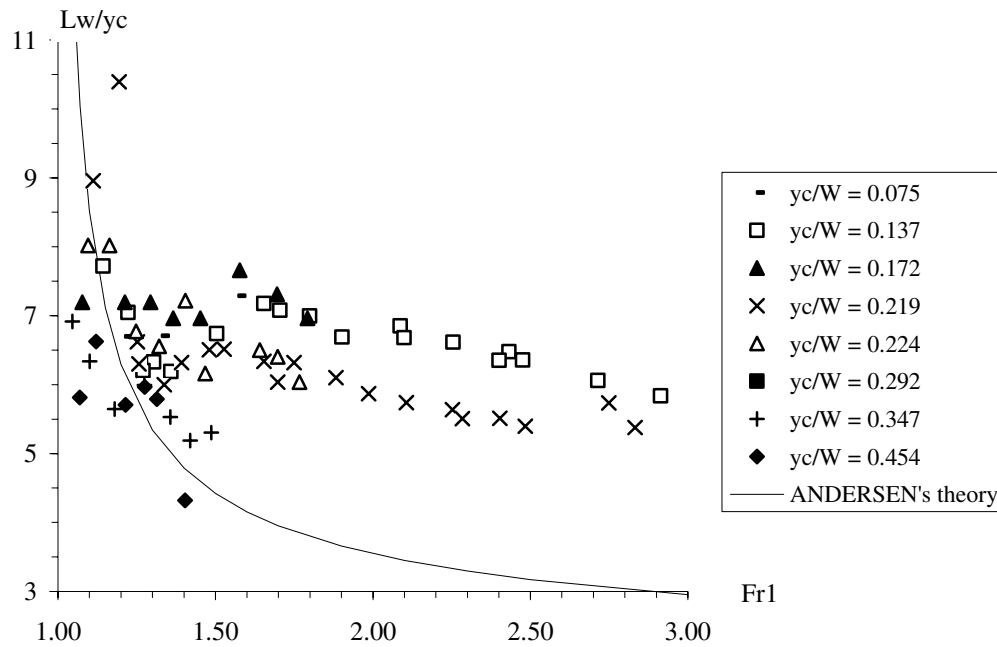
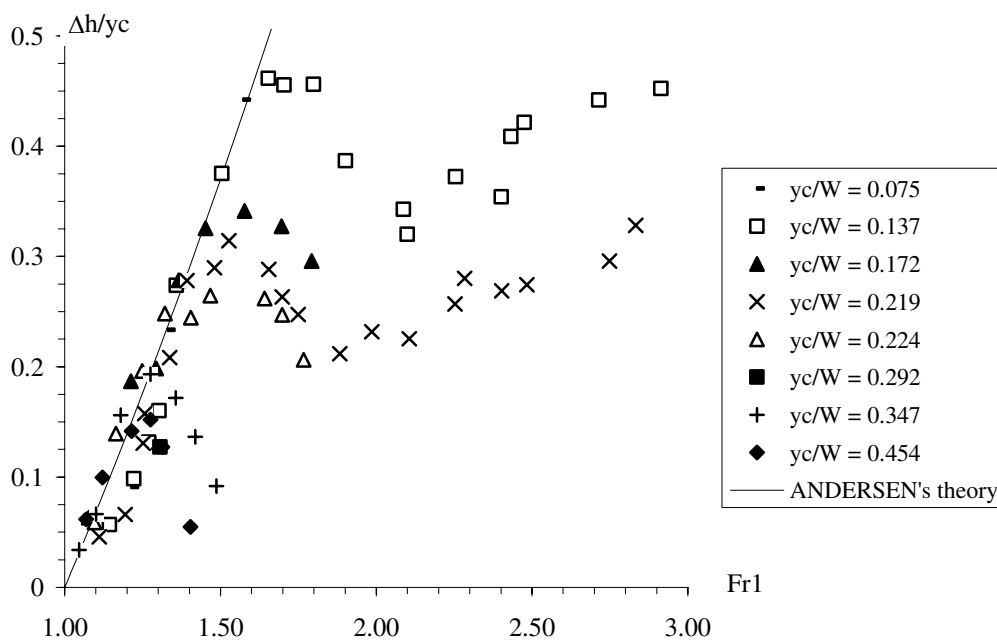


Fig. 10 - Dimensionless wave amplitude $\Delta h/y_c$ as a function of the upstream Froude number (First wavelength)



CHANSON, H., and MONTES, J.S. (1995). "Characteristics of Undular Hydraulic Jumps. Experimental Apparatus and Flow Patterns." *Journal of Hydraulic Engineering*, ASCE, Vol. 121, No. 2, pp. 129-144. Discussion : Vol. 123, No. 2, pp. 161-164 (ISSN 0733-9429).

Fig. 11 - Dimensionless wave length L_w/y_c as a function of the wave length number

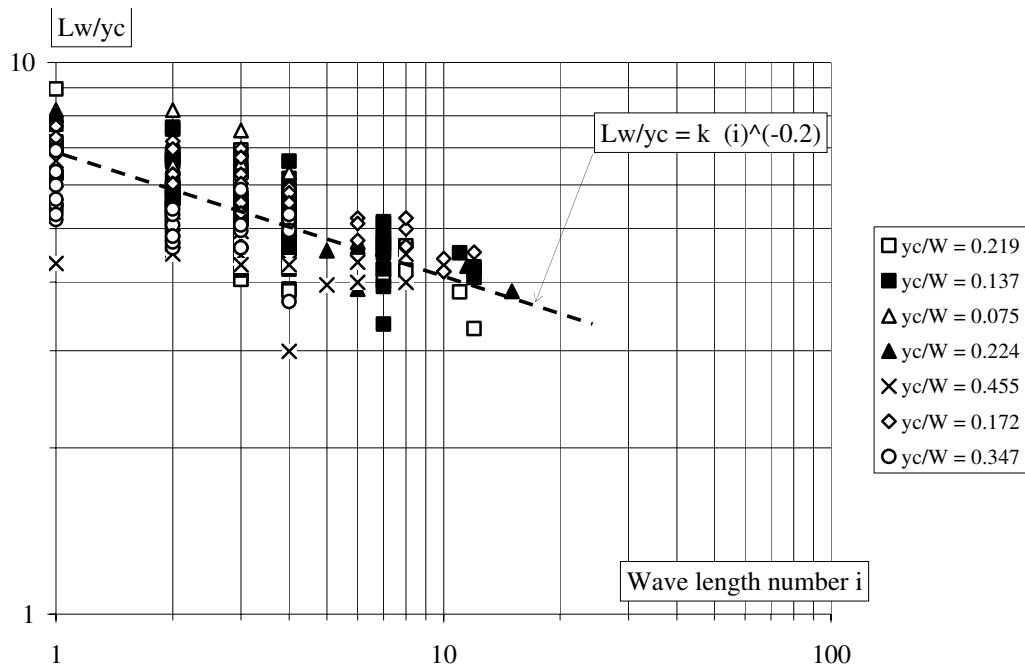
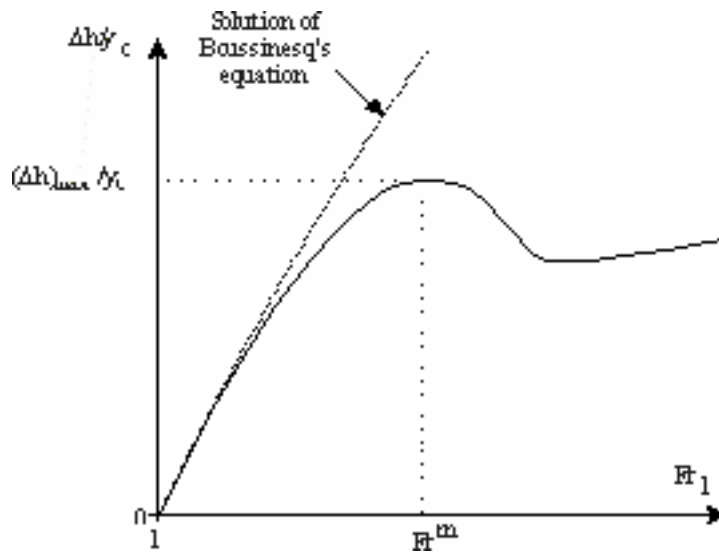


Fig. 12 - Sketch of the dimensionless wave amplitude-upstream Froude number relationship (first wavelength)

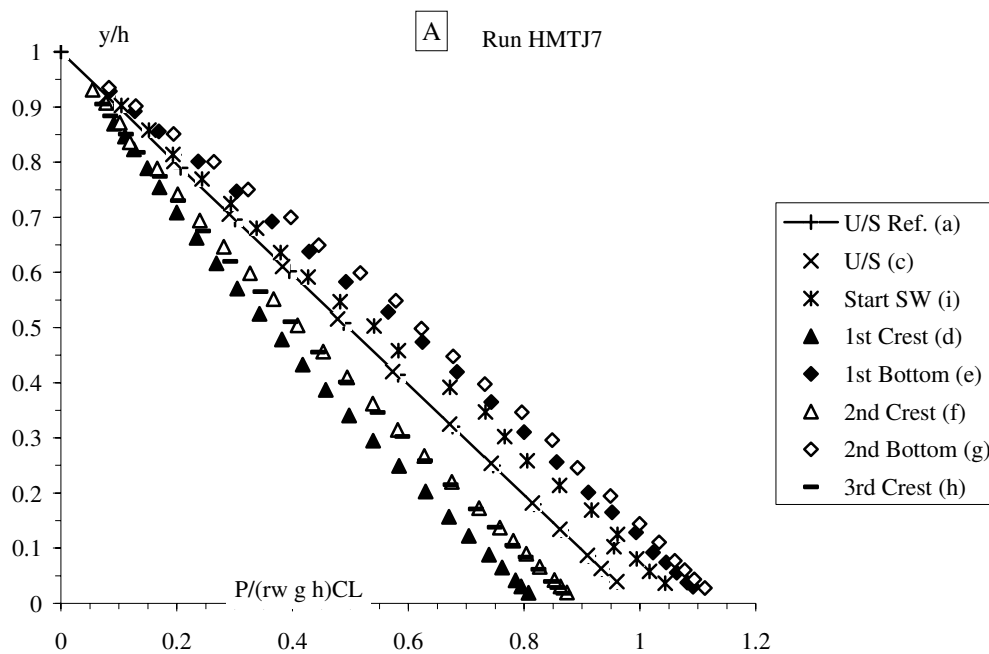


CHANSON, H., and MONTES, J.S. (1995). "Characteristics of Undular Hydraulic Jumps. Experimental Apparatus and Flow Patterns." *Journal of Hydraulic Engineering*, ASCE, Vol. 121, No. 2, pp. 129-144. Discussion : Vol. 123, No. 2, pp. 161-164 (ISSN 0733-9429).

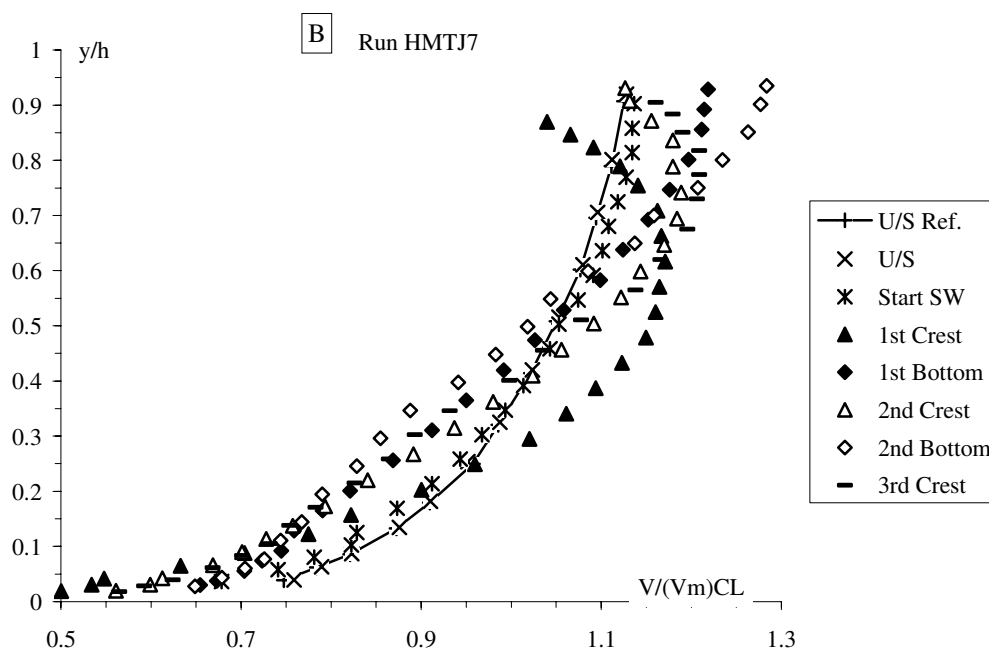
Fig. 13 - Dimensionless distributions along the centreline (undular jump type C)

Run HMTJ7 : $q_w = 0.0399 \text{ m}^2/\text{s}$, $Fr_1 = 1.48$, $y_c/W = 0.218$

(A) Dimensionless pressure distributions $P/(\rho_w g h)_{CL}$



(B) Dimensionless velocity distributions $V/(V_m)_{CL}$



CHANSON, H., and MONTES, J.S. (1995). "Characteristics of Undular Hydraulic Jumps. Experimental Apparatus and Flow Patterns." *Journal of Hydraulic Engineering*, ASCE, Vol. 121, No. 2, pp. 129-144. Discussion : Vol. 123, No. 2, pp. 161-164 (ISSN 0733-9429).

Fig. 13 - Dimensionless distributions along the centreline (undular jump type C)

Run HMTJ7 : $q_w = 0.0399 \text{ m}^2/\text{s}$, $Fr_1 = 1.48$, $y_c/W = 0.218$
 (C) Dimensionless specific energy distributions $E/(E_m)_{CL}$

